Geologica Acta, Vol.15, Nº 4, December 2017, 395-408
DOI: 10.1344/GeologicaActa2017.15.4.9

geologica acta

Zircon and allanite U-Pb ID-TIMS ages of vaugnerites from the Calzadilla pluton, Salamanca (Spain): dating mantle-derived magmatism and post-magmatic subsolidus overprint

F.J. LÓPEZ-MORO[1,2] R.L. ROMER[3] M. LÓPEZ-PLAZA[1] M. GÓNZALEZ SÁNCHEZ[4]

[1]Departamento de Geología, Universidad de Salamanca
37008 Salamanca, Spain.

[2]Salamanca Ingenieros, S.L.
37118 Carbajosa de la Sagrada, Salamanca, Spain.

[3]Deutsches GeoForschungsZentrum (GFZ)
Telegrafenberg, 14473 Potsdam, Germany.

[4]Instituto de Recursos Naturales y Agrobiología de Salamanca (IRNASA-CSIC)
Cordel de Merinas, 40-52, 37008 Salamanca, Spain.

ABSTRACT

Basic to intermediate high-K, high-Mg mantle-derived rocks occur throughout the Iberian Massif and are particularly important in the Tormes Dome, where vaugnerites form several stocks and small plutons. One of the largest and geochemically most variable among these plutons is the Calzadilla pluton in the Tormes Dome that crystallized at 318 ± 1.4Ma (Bashkirian; U-Pb TIMS zircon). This age reveals that the vaugnerite pluton was emplaced during the transition from late D2 extensional deformation to early D3 contractional deformation (319 to 317Ma). Large-scale extension in the area resulted, on one hand, in extensive anatexis in the crust due to quasi-isothermal decompression and mica-dehydration melting and, on the other hand, in the upwelling of the mantle, which induced partial melting of the enriched domains in the lithospheric mantle. The driving reason why crustal and mantle melts were coeval is extension. The U-Pb ID-TIMS age of allanite is not related to the emplacement nor cooling of the Calzadilla vaugnerite, but it seems to be related to a younger subsolidus overprint *ca.* 275Ma that, in the scale of the Central Iberian Zone, corresponds to a period of hydrothermal alteration, including episyenite formation and tungsten mineralization.

KEYWORDS | **Vaugnerite. Zircon. Allanite. U-Pb dating. Subsolidus overprint. Ledesma pluton.**

INTRODUCTION

Vaugnerite was first described by Fournet (1861) in the XIXth century and named after the Vaugneray region, close to Lyon (France). These rocks are dioritic, with a striking (vaugneritic) texture consisting of amphibole and/or decussate, very large biotite crystals protruding in a matrix of plagioclase, amphibole, biotite, alkali feldspar, ± quartz, and ± clinopyroxene as essential constituents, with accessory apatite, zircon, allanite, and titanite. This texture gives the rock a characteristic apparent isotropic fabric.

Typically, vaugnerites form small stocks or occur as enclaves in calc-alkaline and peraluminous leucogranites

that are aligned with shoshonitic series (García de los Ríos, 1981; Sabatier, 1991; López-Moro and López-Plaza, 2001). Vaugnerites are not very important in terms of volume, but occur scattered throughout the entire Variscan Orogenic Belt of Iberia (*e.g.* Gil Ibarguchi, 1982; Sabatier, 1991; López-Moro, 2000; Castro *et al.*, 2003; Gallastegui, 2005; Scarrow *et al.*, 2009; Vegas *et al.*, 2011; Molina *et al.*, 2012; von Raumer *et al.*, 2014).

The particular mineralogy of vaugnerites reflects the high K, LILE, and LREE contents of these rocks at relatively low silica content (intermediate rocks). This particular geochemical signature of vaugnerites and other K-Mg-enriched rocks is obtained from the partial melting of a metasomatically veined mantle, whereas the MgO, Cr, and Mg# as typical mantle signatures reflect that the mantle material and the high contents of K, LILE, and LREE are derived from the metasomes (*e.g.* Foley, 1992; Prelević *et al.*, 2010; 2015). The metasomes represent a material that was originally derived from the subducted slab and its sedimentary cover, and reacted with the mantle above the subducting plate (*e.g.* Prelević *et al.*, 2012; 2015; Soder *et al.*, 2016). The metasomes melted when the thermal structure of the lithospheric mantle changed (*e.g.* Prelević *et al.*, 2010; 2015) and, therefore, the formation of vaugnerite melts may be related to particular tectonothermal events (von Raumer *et al.*, 2014) as, for instance, post-orogenic extension (*e.g.* Janousek and Holub, 2007; Prelević and Foley, 2007).

In the Iberian Massif, vaugnerites are present in Finisterre (Gil Ibarguchi, 1982), the Bayo-Vigo zone (Gallastegui, 2005), Sanabria region (Chacón Muñoz, 2005; Vegas *et al.*, 2011), and the Tormes Dome (García de los Ríos 1981; López-Moro, 2000). Among the vaugnerites of the Central Iberian Zone only those from Bayo-Vigo have been dated (319.6 ± 0.7Ma; Rodríguez *et al.*, 2007). Although the Tormes Dome is the area in the Iberian Massif with the most important occurrences of vaugnerite, *i.e.* there are 6 plutons located in the Sayago region (SW Zamora) and one pluton in the Campo Charro region (Central Northern Salamanca) (Fig. 1); the age of these rocks is only constrained by contact relations. In order to understand the Variscan plutonism in this area, it is important to understand the temporal and genetic relation between the vaugnerites and the surrounding plutonic rocks and, ultimately, the role of the mantle as heat source for crustal melting and as the vaugnerite source. Therefore, in this study, we present U-Pb ID-TIMS zircon and allanite ages to constrain the temporal relationship between vaugnerites and surrounding granitoids.

GEOLOGICAL SETTING

The studied area is part of the Iberian Massif, a large area with Palaeozoic and Ediacaran rocks in western Iberia that have been variably overprinted during the Variscan Orogeny (Fig. 1). The Tormes Dome (TD) represents the southernmost prolongation of the "plutono-metamorphic belts" of the NW Iberian Massif (Fig. 1). The present-day geometry resulted from the superposition of late Variscan structures that controlled the location of zones of extensive partial melting and multiple granite intrusion. The TD composite batholith includes: i) syn-kinematic two-mica granites, including equigranular and porphyritic granites (Fig. 1; López-Plaza and López-Moro, 2004), which are abundant throughout the NW Iberian Massif and known as "Older two-mica Granites" or "Peraluminous Suite" (Capdevila *et al.*, 1973; Castro *et al.*, 2002), and ii) pre/syn-kinematic biotite granitoids and related rocks, with three different associations: IIa) a dioritic-tonalitic association of high-K calc-alkaline affinity; IIb) a granodioritic association, with granodiorites and monzogranites ("Older Granodiorites"), often including spatially, but not genetically, associated vaugnerites and hybrid rocks; and IIIc) a monzonitic association with monzogabbros, monzonites, quartz-monzonites, and scarce monzogranites.

The metamorphic rocks in the TD consist of, from bottom to top:

i) Migmatized felsic gneisses and migmatized Ediacaran-Lower Cambrian sandstones and pelites (the Lower Unit in Escuder Viruete *et al.*, 1994). The felsic gneisses comprise garnet-bearing, fine-grained gneisses and Early Ordovician augen gneisses (López-Moro, 2000; Bea *et al.*, 2006). The migmatized Ediacaran-Lower Cambrian rocks have been partially metamorphosed into garnet-cordierite-biotite-sillimanite paragneisses (Gil Ibarguchi and Martínez, 1982).

ii) Lower Cambrian slates and schists with a low-grade Variscan metamorphic overprint, also known as the Upper Unit in Escuder Viruete *et al.* (1994). These materials represent the highest structural level of the dome. These lithologies are overlain by Ordovician-Silurian platform sediments.

Variscan D1 deformation produced NW-SE trending asymmetric NE-vergent folds in the upper structural levels, and NE-vergent large-scale recumbent folds and thrust sheets in the lower structural levels. D_1 deformation is closely related to Barrovian-type metamorphism at upper amphibolite facies conditions (M1; 700-740ºC and 800-900MPa, Escuder Viruete *et al.*, 2000) that peaked at *ca.* 332Ma (Valverde-Vaquero *et al.*, 2007). Early Variscan compressional structures were variably overprinted during the D2 extensional event, which resulted in a nearly isothermal decompression to a pressure of 300MPa, giving rise to a low-pressure/high-temperature paragenesis (M2), penetrative subhorizontal tectonic

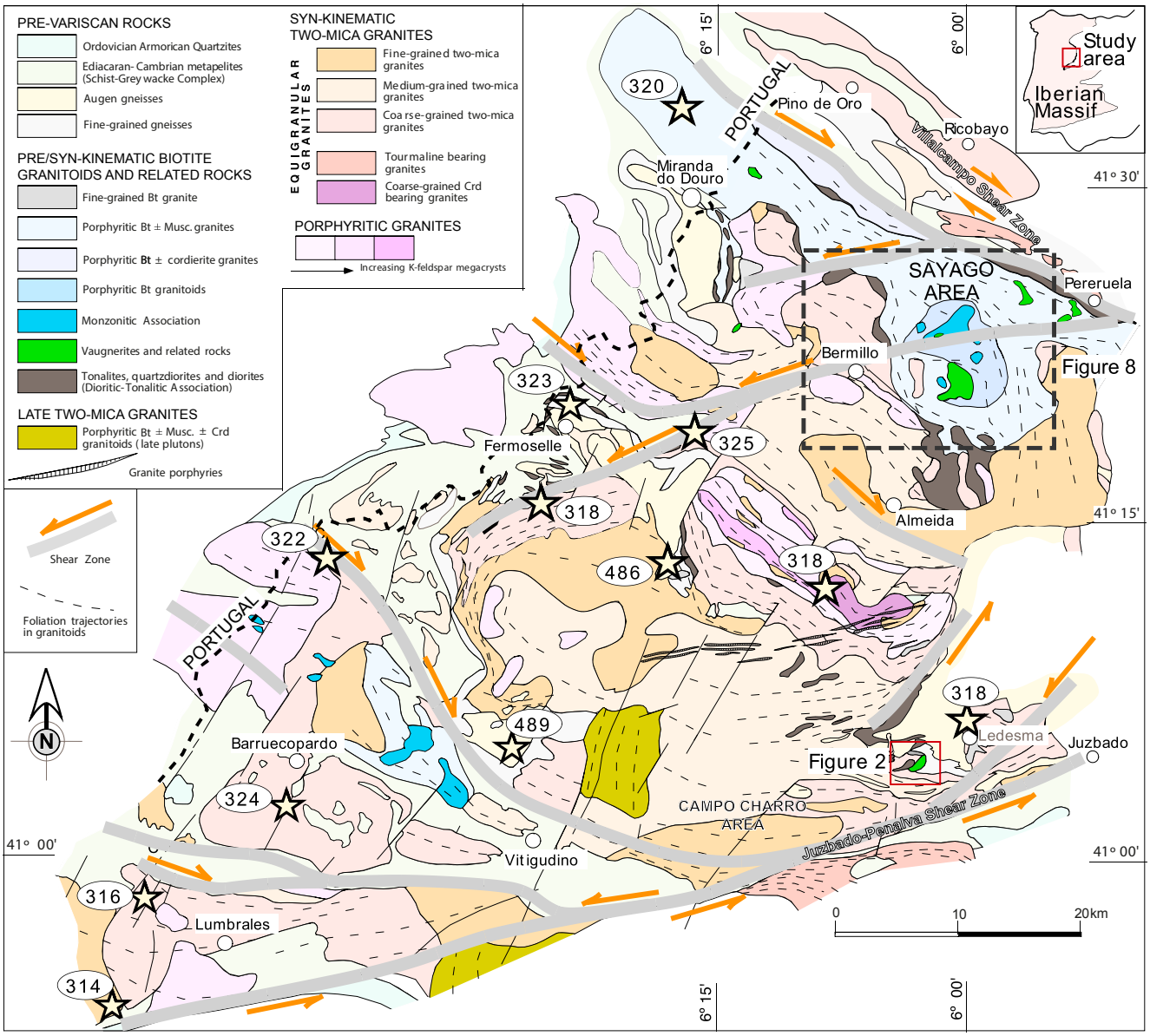

FIGURE 1. Simplified geological map of the Tormes Dome (López-Plaza and López-Moro, 2004), showing the major lithological units, location of vaugnerite plutons and available geochronological data of the Variscan rocks discussed in the text. Augen gneisses ages are after Talavera *et al.* (2013) and granitoid ages after Valverde Vaquero *et al.* (2007), López-Moro *et al.* (2017), and Ferreira *et al.* (2000).

foliation, extensive migmatization and anatexis (Escuder Viruete *et al.*, 1994; 2000). The migmatites yielded ages at 325-320Ma (Valverde-Vaquero *et al.*, 2007). The third deformational phase (D3) was the consequence of NNE-SSW compression (Iglesias and Choukroune, 1980; López Plaza, 1982), which resulted in i) subvertical to moderately NE-vergent synforms and antiforms, and ii) strike-slip shear zones, being the sinistral Juzbado-Penalva Shear Zone (Fig. 1) the most prominent of them. Voluminous syn-D3 granitoids yield ages at 316–310Ma (Valverde-Vaquero *et al.*, 2007; López-Moro *et al.*, 2012), whereas sinistral movements along the Juzbado-Penalva Shear Zone and the Villalcampo Shear Zone have been dated at 309Ma and 306 ± 3Ma, respectively (using the $^{40}Ar/^{39}Ar$ method, Gutiérrez-Alonso *et al.*, 2015).

The vaugneritic Calzadilla pluton

The vaugneritic Calzadilla pluton is a small NE-SW elongated pluton of a length of 2.5km and a width of around 600m (López-Plaza *et al.*, 2007; Fig. 2). The pluton is surrounded by two-mica leucogranites that locally crosscut the external contact of the pluton, although the contacts between these rocks generally are

concordant. Based on mineral association, texture, and grain size distribution, different facies of vaugnerites *s.s.* and associated intermediate rocks have been distinguished (Fig. 3) (see González Sánchez, 2016): a) fine-grained intermediate rocks without vaugnerite texture; b) mesocratic biotite - amphibole vaugnerite; c) leucocratic biotite - amphibole vaugnerite, and d) leucocratic biotite ± amphibole vaugnerite. Fine-grained facies surrounds vaugnerites *s.s.* to the NE, SW and SE and locally also to the NW (Fig. 2). Vaugnerites *s.s.* display zoning at pluton scale, consisting of different compositional bands close to the NE-SW direction. The zoning ranges from the least evolved mesocratic facies to the East-Southeast, to the most evolved facies to

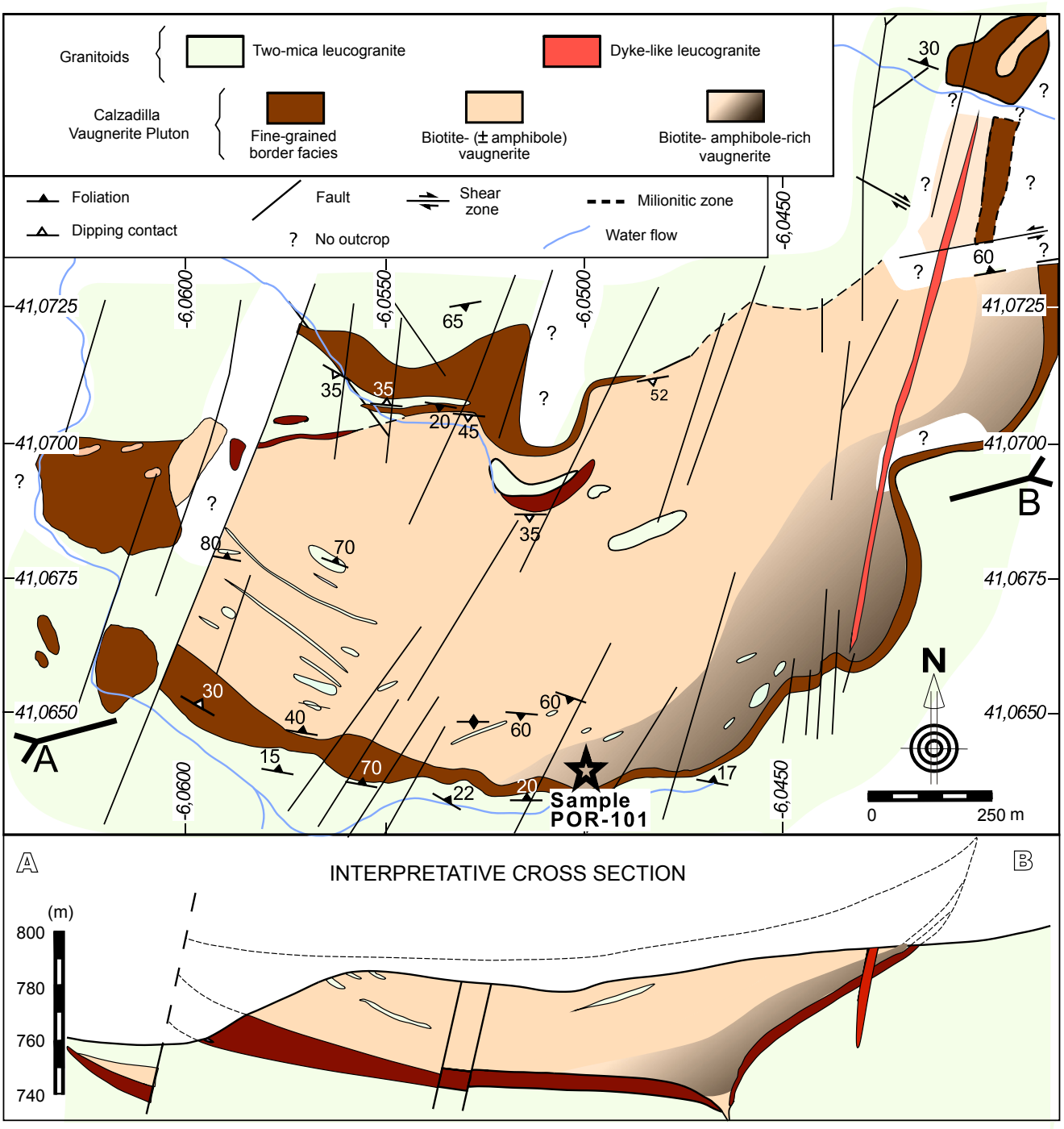

FIGURE 2. Geological map of the Calzadilla Pluton (above) and interpretative cross section (below, modified from González Sánchez, 2016). The location of the sample used for dating is marked by a star (UTM coordinates, X: 747.913; Y: 4550.010; Zone 29, Datum: ETRS89).

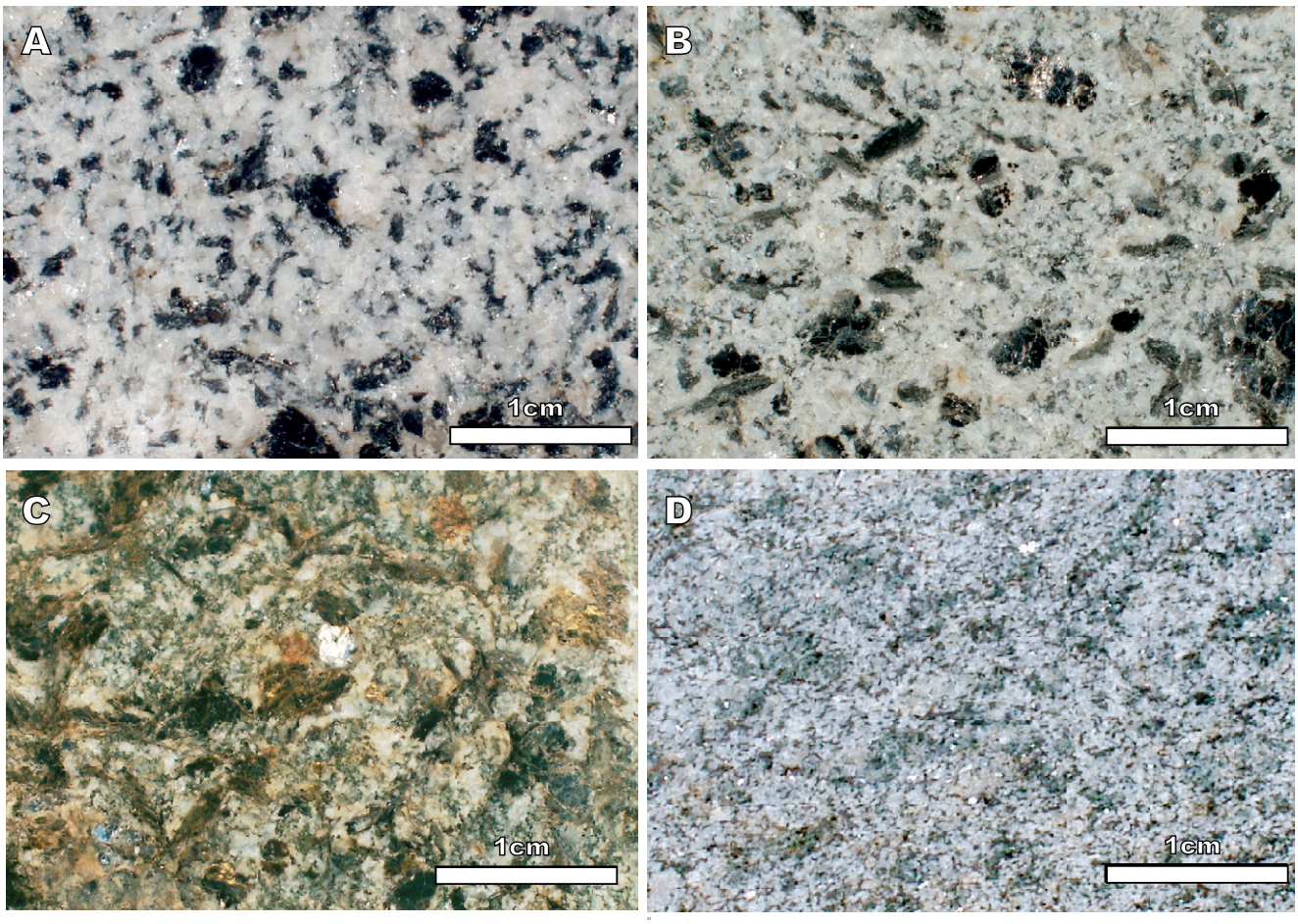

FIGURE 3. A-C) Hand specimens of vaugnerites *s.s.* and associated rocks. A) Leucocratic biotite ± amphibole vaugnerite; B) leucocratic biotite - amphibole vaugnerite; C) mesocratic biotite - amphibole vaugnerite; D) fine-grained intermediate facies without vaugnerite texture (border facies).

the West, largely reflecting the depletion in amphibole (Fig. 2). The leucocratic biotite ± amphibole vaugnerite is the most abundant facies, and the mesocratic rocks are the least abundant facies and tend to occur in meter-scale boulders (Fig. 4). The peripheral fine-grained facies or border facies displays a marked strain anisotropy parallel to the exo-contact. Both foliation and exocontact show a centripetal pattern, with different dip directions in the South and the North of the pluton, reflecting a lopolith-like body (Fig. 2) In contrast, the geometry of the vaugnerite *s.s.* facies displays an internal pattern, which appears to be, to a certain extent, independent of the border facies, showing an upwards magmatic differentiation, as it can be inferred by the progressive decrease in amphibole (Fig. 2). Both types of facies, despite being presumably coeval, manifest two different prevailing effects: the early magmatic pulse of the border facies absorbed the deformational strain at the floor of the pluton, whereas the subsequent internal vaugneritic facies accommodated the magmatic evolution inside the pluton. Consistently, this pattern seems to account for a two-stage construction of the lopolith-like body with a steep feeder conduit located at the SE part of the pluton (Fig. 2).

PETROGRAPHY DESCRIPTION

Vaugnerites from the Calzadilla pluton (in Ledesma pluton) and other vaugnerites from the Tormes Dome consist of amphibole, biotite, plagioclase, quartz and interstitial K-feldspar as major components, whereas apatite is the most characteristic accessory mineral (López-Moro, 2000). Less common accessory minerals are zircon, allanite, monazite, titanite, epidote, magnetite-hematite, chalcopyrite and pyrrhotite. The most distinctive feature of the vaugnerites is their decussated texture, defined by large crystals of biotite and amphibole (Fig. 3A; B; C).

Plagioclase is the most abundant mineral, ranging between 31 and 41% in volume. It forms up to 4mm large crystals, corresponding texturally to the "complex plagioclase phenocrysts" (A-Type) of Sabatier (1991). There is a large difference in the anorthite content between

FIGURE 4. Outcrop photograph showing the characteristic boulders of leucocratic biotite - amphibole vaugnerite at the sampling site. The picture was taken in an E-W direction and looking eastwards.

the partially resorbed cores (An_{67-55}) and the non-resorbed part of these phenocrysts. The composition of the latter plagioclase shows a relatively small variation (An_{35-25}), being similar to the one of small (<600μm) plagioclase phenocrysts and abundant plagioclase crystals in the groundmass, which suggests simultaneous crystallization. Rims and matrix plagioclase correspond to the B-Type of Sabatier (1991).

The amphibole occurs as isolated crystals of 100-400 microns, sometimes hosting small crystals of clinopyroxene, or in millimeter polycrystalline clots consisting of amphibole, or amphibole, sulphides and biotite (López-Moro and López-Plaza, 2004a). Amphibole modal content ranges between 0.1% (in leucocratic biotite ± amphibole vaugnerites) and 19.7% (in mesocratic biotite – amphibole vaugnerites, González Sánchez, 2016). Compositionally, vaugnerite *s.s.* amphiboles are magnesio-hornblende and, occasionally, actinolite (López-Moro and López-Plaza, 2004a).

There are three types of biotite, which is rather abundant as phenocryst and in the matrix (15-29 vol.%): a) large poikilitic, up to 5mm crystals, hosting apatite, plagioclase, clinopyroxene, amphibole and, locally, allanite; b) small tabular crystals (100-200μm), associated with amphibolic clots; and c) very small rounded crystals (≈10μm), hosted by plagioclase (López-Moro, 2000).

K-feldspar occurs either as an interstitial phase or as a component of up to 4mm-large ocelli. Its abundance varies between 5.7 and 17.1 vol.%, from dark to light rocks, respectively. K-feldspar is dominantly orthoclase (rarely adularia), as indicated by its monoclinic symmetry and 2Vx angle values of between 52° and 74° (López-Moro and López-Plaza, 1998).

Clinopyroxene typically forms euhedral or subhedral 400-800μm-sized crystals. It is relatively uncommon (0.68-2 vol.%) and generally absent in the most differentiated samples. Present as diopside ($En_{37-38}Fs_{13.9-15.6}Wo_{47-48.7}$;

López-Moro, 2000), it is similar to the clinopyroxene from the vaugnerites of the French Central Massif (Michon, 1987; Sabatier, 1991).

Allanite is a common accessory mineral in the various vaugnerite types. Its modal content is always <1%. It commonly exhibits crystal zoning, as well as a conspicuous alteration that is also recorded in biotite crystals with a marked chloritization (Fig. 5). Apatite is always present as fluorapatite. In melanocratic vaugnerites, it forms small crystals, whereas in leucocratic vaugnerite it occurs as larger crystals, typically rounded. Titanite is irregularly distributed and may locally reach high amounts (>1% in vol.), particularly in association with mafic minerals, such as amphibole and biotite. A local enrichment may reflect a secondary origin of titanite resulting from the redistribution of Ti from mafic minerals. Ilmenite is the major Ti-phase in amphibole-free quartzmonzonite, where it is abundant and occurs as inclusions in biotite and, less commonly, in the groundmass. Zircon usually occurs in euhedral grains (Fig. 5), ranging between 250 to 100 microns and, in most cases, is hosted in large biotite crystals. Nevertheless, the largest crystals are presented together with framework silicates.

METHODS

Zircon and allanite concentrates were obtained from a leucocratic biotite - amphibole vaugnerite (Figs. 2 and 4) by using the Wilfley table, Frantz isodynamic magnet separator, and heavy liquids (bromoform and methylene iodide). Inclusion-free, perfectly clear zircon crystals were selected under the binocular microscope. Before dissolution, zircon was rinsed in warm 7N HNO_3 to remove U attached to the mineral surface, and cleaned in warm H_2O and acetone. Zircon and a ^{205}Pb-^{235}U mixed tracer were weighted into small teflon vials. The spike solution was dried before the addition of concentrated HF. The vials were put in a Parr autoclave and the zircon was dissolved at 210°C for four days. After drying the samples, zircon was redissolved in 6N HCl in the autoclave at 210°C overnight. After the samples had been dried again and taken up in 3N HCl, Pb and U were separated using the ion-exchange chromatography procedure described by Krogh (1973).

Allanite and a ^{205}Pb-^{235}U mixed tracer were weighted in screw-top beakers and dissolved using concentrated HF overnight on a hot plate at 140-160°C. Lead and U were separated using HCl-HBr ion-exchange chromatography and U was cleaned using the HNO_3-HCl ion-exchange chromatography procedure described in Baumgartner *et al.* (2006).

Pb and U were loaded together on single Re-filaments using a silica-gel emitter and H_3PO_4 (Gerstenberger and Haase, 1997), and measured at 1200°-1260°C and 1350-1400°C, respectively, on a Finnigan MAT262 multi-collector mass-spectrometer using Faraday collectors and ion counting. Geochronological data plotting were performed using the Isoplot program of Ludwig (2000).

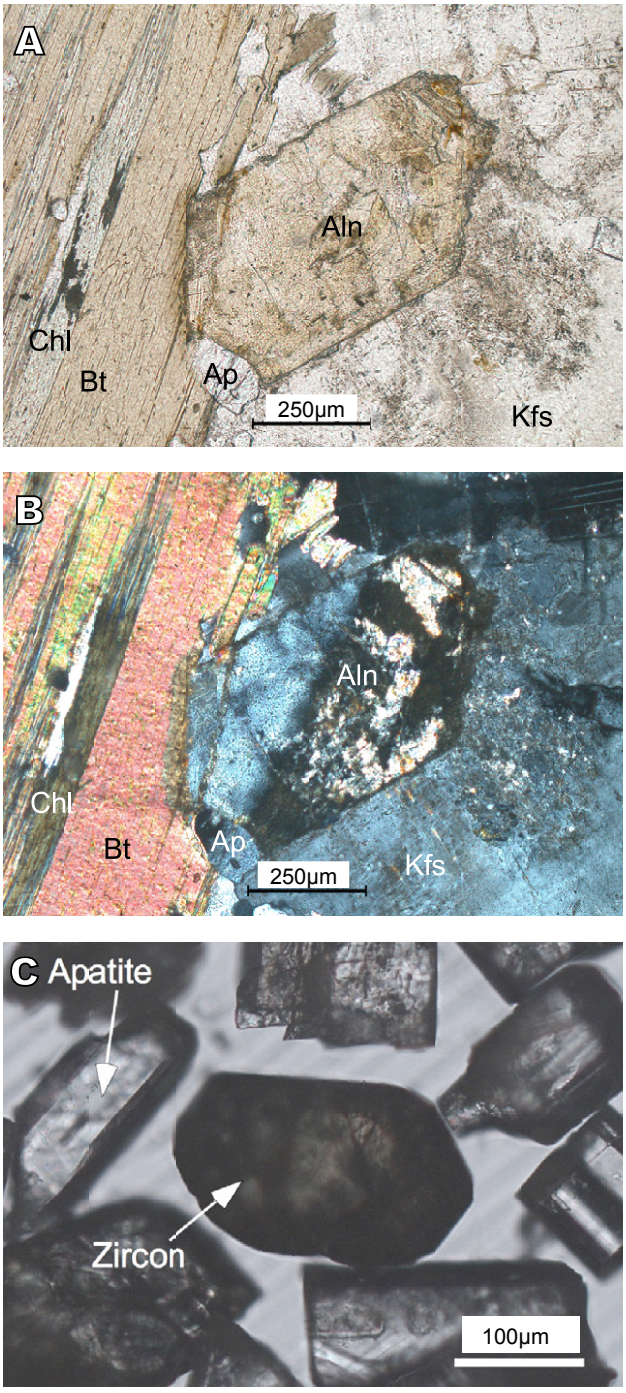

FIGURE 5. Microphotographs of dated minerals. A) Allanite with alteration in plane light and B) crossed polars; C) mineral concentrate with an euhedral zircon grain and abundant apatite crystals (plane-line view). Mineral abbreviations are after Whitney and Evans (2010).

RESULTS

Six multi-grain zircon samples were analyzed. Care was taken to select only clear crystals, free of inclusions and fractures. Zircons from these fractions show a broad range of U contents from 213 to 1,236ppm (Table 1). Five fractions are concordant and one is slightly discordant (Fig. 6). Four fractions overlap within the error and define a weighted $^{206}Pb/^{238}U$ age of 318.1 ± 1.4Ma (2σ; Fig. 6). The remaining two samples are shifted to slightly lower $^{206}Pb/^{238}U$ ages and were not used for age calculation. The slight offset of the two samples to a younger age is interpreted as due to a minor Pb-loss. As the dated zircon does not show any indication of inheritance, the age of 318.1 ± 1.4Ma is interpreted as the age of the vaugnerite emplacement.

The analyzed allanite samples have markedly lower U content (130 to 186ppm) and markedly higher Pb content (113 to 198ppm) than zircon (compare Table 2 with Table 1). Most of the Pb in allanite is common Pb. Therefore, the measured $^{206}Pb/^{204}Pb$ and $^{207}Pb/^{204}Pb$ ratios are not very radiogenic ($^{206}Pb/^{204}Pb$ ranges from 23.07 to 44.12; Table 2), and the calculated $^{206}Pb/^{238}U$ and $^{207}Pb/^{235}U$ ratios have large uncertainties, in part due to uncertainties in the common Pb composition, and also due to the limited formation of radiogenic Pb. Therefore, the allanite samples are not shown in a concordia diagram. Instead, they are shown in the $^{206}Pb/^{204}Pb$ *vs.* $^{238}U/^{204}Pb$ diagram (Fig. 7). The allanite samples scatter about a reference line of 275Ma, *i.e.* they all fall below the reference line of 318Ma, which corresponds to the U-Pb zircon age and represents the best age estimate for the emplacement of the vaugnerite. In the $^{206}Pb/^{204}Pb$ – $^{207}Pb/^{204}Pb$ diagram (not shown), the allanite samples fall on a straight line with some excess scatter. Because of their high Th/U ratio (Table 2), the various allanite samples may show excess of ^{206}Pb. Excess of Pb originates from ^{230}Th, which is part of the ^{238}U decay series. Minerals that strongly favor Th over U incorporate significantly more ^{230}Th than they would if ^{230}Th and ^{238}U were in activity equilibrium. The surplus of ^{230}Th eventually results in an excess of ^{206}Pb (Schärer, 1984). Correction of excess of Pb, however, is too insignificant to remove the scatter in the $^{206}Pb/^{204}Pb$ *vs.* $^{238}U/^{204}Pb$ diagram, and would reduce the age rather than increase it. As textural relations demonstrate that allanite is a magmatic phase, the U-Pb systematics of allanite implies that it has been disturbed by a younger event, which may have resulted in partial or complete resetting of the U-Pb system of allanite.

DISCUSSION

Magmatism and tectonic activity at the time of the emplacement of vaugnerite in the Tormes Dome

Multiple evidences demonstrate that in the Tormes Dome magmatism and tectonic activity are closely related. For instance, the older granodiorites from the Sayago area, leucogranites from the Ledesma area and small vaugnerite plutons from both areas – despite their contrasting chemical composition – were emplaced at the same time as indicated by mingling structures (*e.g.* ocelli) and lobulated contacts between vaugnerites and their host granitoids. These different plutonic rocks have all been affected by the same deformational stage (D2 phase), which resulted in a subhorizontal foliation that is concordant both in vaugnerites and host granitoids (López-Plaza *et al.*, 2012). The D2 tectonic phase in the area has been dated using migmatites (325-320Ma, Valverde-Vaquero *et al.*, 2007) that are related to this tectonic phase, as they show a subhorizonal foliation, which is a typical feature of D2, and that were later folded by the D3 phase. The tectonic constraints derived from migmatite dating are in line with the available age data from the oldest granodiorite of the Sayago area, dated at 320 ± 5Ma (U-Pb in monazite; Ferreira *et al.*, 2000) and the *ca.* 320Ma age of vaugnerites from the Sayago area inferred by structural relations

TABLE 1. U-Pb analytical data of zircons from Calzadilla vaugnerite pluton (leucocratic biotite - amphibole vaugnerite)

Sample	Weight (mg)	Concentrat. (ppm)		$^{206}Pb/^{204}Pb$ Measured ratios[a]	Common Pb (pg)	Radiogenic Pb (at%)[b]			Isotopic ratios[b]					Apparent ages (Ma)[c]		
		U	Pb_{tot}			^{206}Pb	^{207}Pb	^{208}Pb	$^{238}U/^{204}Pb$	$^{206}Pb/^{238}U$	$^{207}Pb/^{235}U$	$^{207}Pb/^{206}Pb$	Error Correl.	$^{206}Pb/^{238}U$	$^{207}Pb/^{235}U$	$^{207}Pb/^{206}Pb$
1	0.084	1003	57.2	518.8	531	84.85	4.48	10.66	10000	0.04998(0.6)	0.36400(0.7)	0.05282(0.5)	0.78	314	315	321
2	0.097	964	53.1	848.0	359	84.80	4.49	10.71	16400	0.05049(0.6)	0.36816(0.7)	0.05289(0.3)	0.89	318	318	324
3	0.064	1040	55.5	1226	175	85.51	4.52	9.97	23900	0.05046(0.4)	0.36783(0.5)	0.05287(0.3)	0.73	317	318	323
4	0.075	1236	64.0	1498	200	87.78	4.64	7.58	29200	0.05069(0.3)	0.36947(0.4)	0.05287(0.3)	0.80	319	319	323
5	0.113	1101	56.6	1377	288	87.27	4.62	8.11	27300	0.04982(0.4)	0.36375(0.4)	0.05295(0.2)	0.87	313	315	326
6	0.210	213	12.0	752.8	196	84.50	4.46	11.05	14400	0.05083(0.9)	0.36971(1.0)	0.05275(0.4)	0.93	320	320	318

[a] Lead isotope ratios corrected for fractionation (0.1% /a.m.u.).

[b] Lead corrected for fractionation, blank, tracer contribution, and initial lead with $^{206}Pb/^{204}Pb = 17.6±0.3$, $^{207}Pb/^{204}Pb = 15.55±0.05$, $^{208}Pb/^{204}Pb = 38.1±0.3$.
During the measurement period; total blanks were less than 15pg for lead and less th an 1 pg for uranium. Errors on the isotop ic ratios (values in brackets) at 2-sigma level (%).

[c] Apparent ages were calculated using the constants recommended by IUGS (Steiger and Jäger 1977).

TABLE 2. U-Pb analytical data of allanite from Calzadilla vaugnerite pluton (leucocratic biotite - amphibole vaugnerite)

Sample	Weight (mg)	Concentrations (ppm)		Common Pb (pg)	Isotopic ratios[a]				
		U	Pb_{tot}		$^{206}Pb/^{204}Pb$	$^{207}Pb/^{204}Pb$	$^{208}Pb/^{204}Pb$	$^{238}U/^{204}Pb$	$^{232}Th/^{238}U$
1	0.122	161	117	2790	39.204	16.767	317.00	444.00	40.5
2	0.077	150	113	1200	44.115	16.972	453.00	592.00	49.1
3	0.094	130	119	4100	27.538	16.109	154.50	189.1	36.8
4	0.137	178	182	13800	23.529	15.899	91.28	110.9	28.2
5	0.052	157	198	5750	23.074	15.891	90.39	89.58	30.0
6	0.042	186	128	1400	33.187	16.341	225.00	348	37.7

[a] Concentrations determined by isotope dilution using a mixed ^{205}Pb-^{235}U tracer.

[b] Lead isotope ratios corrected for isotopic fractionation (0.1% / a.m.u.), blank and tracer contribution. Analytical uncertainties at 2-sigma level are better than 0.1% for Pb isotope ratios, and 1% for $^{238}U/^{204}Pb$.

[c] Calculated for an age of 275Ma using $^{208}Pb\ rad/^{206}Pb\ rad$ (estimated using measured $^{206}Pb/^{204}Pb$ and $^{208}Pb/^{204}Pb$, corrected for common lead with $^{206}Pb/^{204}Pb = 17.6$ and $^{208}Pb/^{204}Pb = 38.1$).

between vaugnerites and the granodiorite of the Sayago area, suggesting that both melts were coeval (López-Moro, 2000). Similar conclusions can be drawn from the ages of the Calzadilla pluton (this work, U-Pb in zircon, 318.1 ± 1.4Ma), the Bayo-Vigo vaugnerite age in the Iberian Massif (U-Pb in zircon; 319.6 ± 0.7Ma, Rodríguez *et al.*, 2007) and the vaugnerite age in Sanabria (U-Pb in titanite, 317 ± 1Ma, Vegas *et al.*, 2011). The vaugnerite age data demonstrate that these melts were emplaced broadly simultaneous over a very large part of the Iberian Massif.

In the Campo Charro area, where the Calzadilla pluton outcrops, the age of vaugnerites coincides with the emplacement ages of local granitoids, *i.e.* coarse-grained two-mica granites in Ledesma (318.2 ± 1.8Ma, zircon U-Pb LA-ICP-MS; López-Moro *et al.*, 2017), calc-alkaline affinity biotite-granitoid in Ledesma (318.3 ± 2.5Ma, zircon U-Pb LA-ICP-MS; López-Moro *et al.*, 2017) and cordierite-bearing granites in the Pelilla complex (318.3 ± 1Ma, zircon U-Pb LA-ICP-MS; López-Moro *et al.*, 2017) (Fig. 1). The same age also has been reported in S-type granites from the nearby Penedono Massif in Portugal (318.7 ± 4.8Ma; Pereira *et al.*, 2017). This latter age is thought to date the final activity of D2 extensional shear and the onset of D3 contractional deformation (Pereira *et al.*, 2017).

These geochronological data highlight the importance of coeval crustal (granites, migmatites) and mantle (vaugnerite) melts during the final stages of D2, and the onset of D3 in the Iberian Massif. This spatial and temporal coincidence raises the question whether vaugnerite and crustal melts are petrologically related or whether their formation is controlled by a common cause. Although vaugnerites have high liquidus temperatures, between 1200ºC and 1050ºC (López-Moro, 2000), it is unlikely that vaugnerite melts represent the heat source of crustal melting, as: i) vaugnerite plutons are volumetrically insignificant in comparison to the huge amount of granites in the Tormes Dome, and ii) gravimetric data show that the vaugnerites are small stocks or pipe-like bodies and that there are not big magma chambers at depth (Fig. 8).

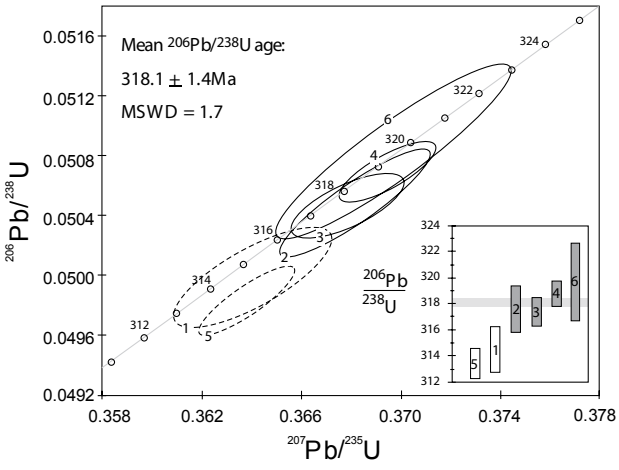

FIGURE 6. Concordia diagram for zircons from the Calzadilla vaugnerite pluton (amphibole-bearing biotite vaugnerite facies). Fractions represented as dashed ellipses were not used for age calculation. The inset shows the $^{206}Pb/^{238}U$ ages of the various fractions. Grey fractions were used to calculate weighted average $^{206}Pb/^{238}U$ age.
MSWD = mean square of weighted deviates.

The coeval occurrence of crustal and mantle melts, however, may be causally related to the D2 extension in the Tormes Dome. In the crust, D2 extension resulted in quasi-isothermal decompression (Escuder Viruete *et al.*, 1994), allowing for mica-dehydration partial melting and

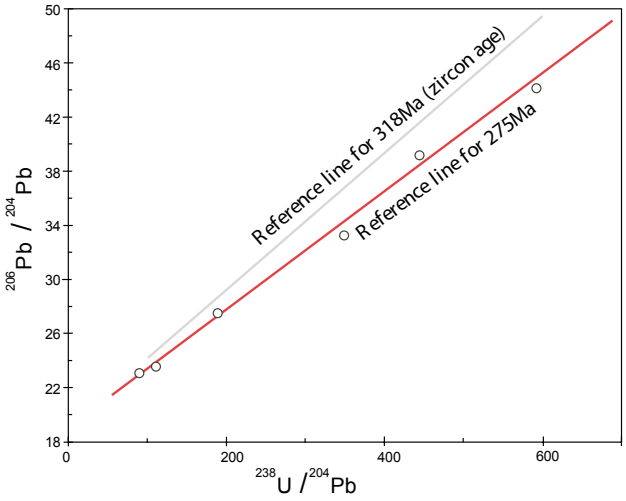

FIGURE 7. $^{206}Pb/^{204}Pb$ - $^{238}U/^{204}Pb$ diagram showing allanite samples scattering around a reference line of 275Ma. Line of 318Ma (zircon age) is shown as a reference.

the formation of migmatites and two-mica granites in the area (López-Moro *et al.*, 2012). In the mantle, the thinning of the crust by extension favors the upwelling of the mantle and adiabatic melting of metasomatic domains that represent the source of vaugnerite melts. In such a scenario of strong decompression, crustal- and mantle-derived melts are coeval. Furthermore, D2 extension also accounts for the subhorizontal foliation developed in vaugnerites.

Post-magmatic alteration event dating

One of the most striking features of the vaugnerites in the Calzadilla pluton is the low apparent emplacement temperature (average 537ºC) and pressure (90MPa) obtained using geothermometers (*i.e.* Pl-Kfs, Pl-Amp, Ti in Amph, Cpx; see López-Moro *et al.*, 1998; López-Moro and López-Plaza, 2004a, b) and geobarometers (amphibole composition; López-Moro and López-Plaza, 2004a). These estimates are distinctly lower than typical magmatic values, suggesting subsolidus re-equilibration with a fluid phase present either during late-stage magmatic crystallization or during a later unrelated event. Faults or strike-slip faults commonly channel available fluids (*e.g.* McCaig, 1988; McCaig *et al.*, 1990; Selverstone *et al.*, 1991; Streit and Cox, 1998), which may result in late re-equilibration of minerals in permeable units and may record the long-lived history of fluid flow and alteration.

Excess scatter and a high common Pb content in allanite do not favor complete resetting. Instead, the excess scatter may be explained by: i) heterogeneity of the common Pb

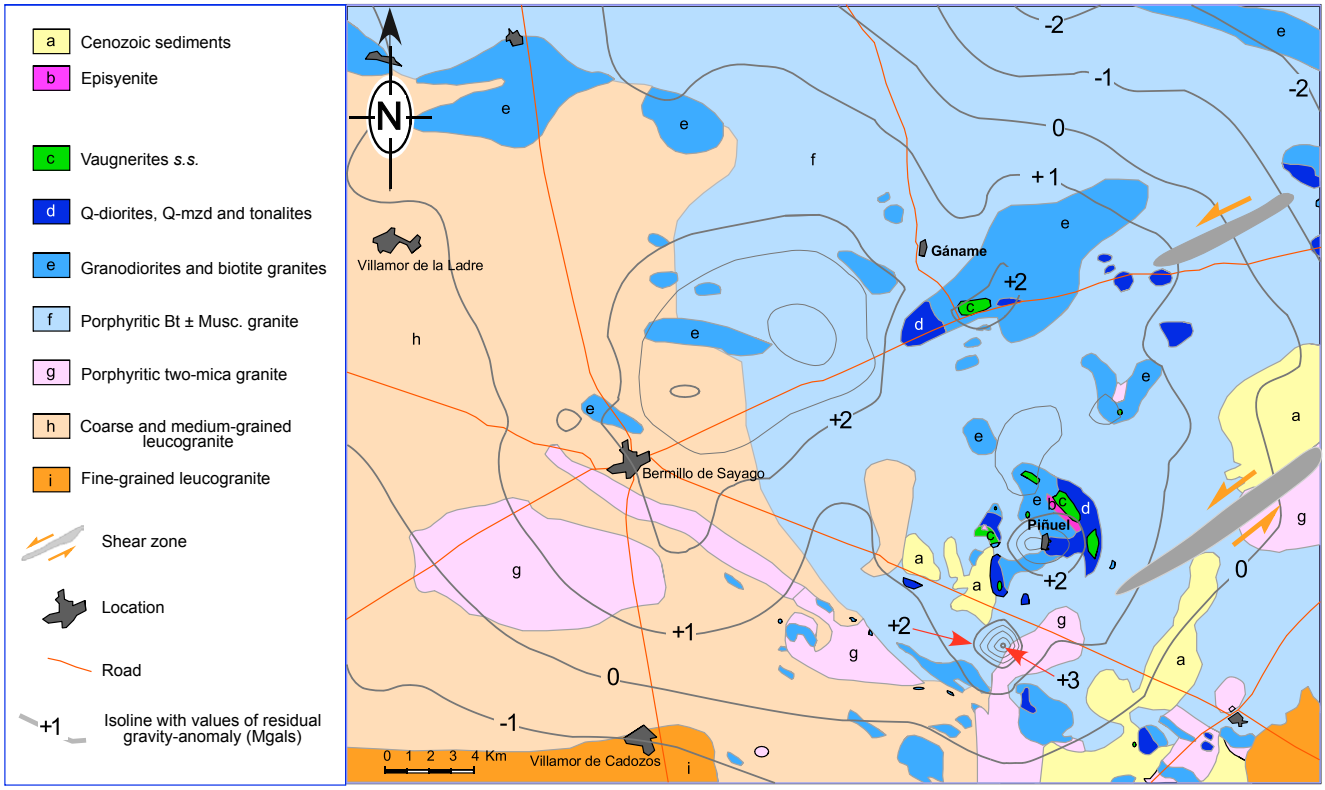

FIGURE 8. Residual gravity map of the Sayago area (López-Plaza and López-Moro, 2008). Note the strong positive anomaly related with the vaugnerite plutons near Piñuel and Gáname, and the episyenites in the vaugnerite pluton near Piñuel.

isotopic composition (Pb initially incorporated or added during alteration), or ii) partial loss of common and radiogenic Pb that does not affect all allanite samples to the same extent. Thus, the reference line in the $^{206}Pb/^{204}Pb$ *vs.* $^{238}U/^{204}Pb$ diagram (Fig. 7) gives a rough estimate of the maximum age of disturbance.

Note that an age discrepancy between the U-Pb ages of magmatic zircon and allanite from the same rock also has been reported by Poitrasson (2002) for rocks in Sardinia. Alteration of allanite seems to result in the loss of LREE, the addition of common Pb (actually, any available Pb) and, possibly, local redistribution of Th (Poitrasson, 2002). This alteration may be supported by metamictization of the allanite crystal lattice, which becomes increasingly more important as the mineral becomes older. Actually, the observation that the alteration of allanite may facilitate the incorporation of Pb (Poitrasson, 2002) implies, that the high common Pb content in allanite from the Calzadilla vaugnerite (Table 2) is not necessarily magmatic but, at least in part, was acquired during its alteration.

Close to the Ledesma pluton there was an important fluid flow associated with the sinestral Juzbado-Penalva Shear Zone and associated branches, which has been interpreted to reflect the beginning of crustal extension (González-Clavijo and Díez Montes, 2008) (Fig. 1). Ductile deformation along this mega structure has been dated at 309Ma ($^{40}Ar/^{39}Ar$ method; Gutiérrez-Alonso *et al.*, 2015), whereas the age of younger reactivations as normal faults is not known (González-Clavijo and Díez Montes, 2008). In the conjugate Villalcampo Shear Zone (Fig. 1) ductile deformation has been dated ($^{40}Ar/^{39}Ar$ in micas; 306 ± 3Ma; Gutiérrez-Alonso *et al.*, 2015), and gold-bearing episyenites that formed at 420ºC in relation to fluid flow yielded younger ages (chemical ages in uraninites, 270 ± 12Ma, López-Moro *et al.*, 2013), highlighting the recurrent reactivation of these structures, which clearly also affected vaugnerites in the Tormes Dome (Figs. 1 and 8) over a long period. This younger age agrees well with the ages of barren episyenites from the Spanish Central System (SCS), that gave Rb-Sr internal isochrons with an age of *ca.* 274 ± 6Ma (Caballero *et al.*, 1993). Similarly, young hydrothermal activity along faults is also known thanks to quartz veins containing scheelite-wolframite in the Barruecopardo district (287 ± 5Ma; K-Ar in muscovites; Antona, 1991) and scheelite-bearing quartz veins from El Cabaco in the SCS (277-287 ± 20Ma, chemical ages in uraninites; López-Moro *et al.*, 2007). This abundance of ages around 280Ma (Fig. 9) indicates that the U-Pb allanite age is likely to represent a geologically significant event of resetting of the U-Pb system.

Fluids that re-equilibrated essential minerals in vaugnerites could have also disturbed the composition

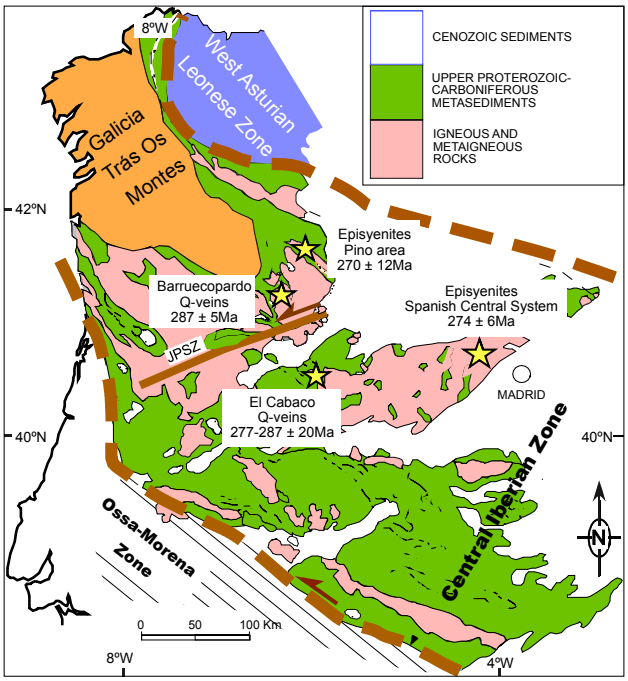

FIGURE 9. Location of Permian hydrothermal deposits and metasomatic rocks in the Iberian Massif. Stars correspond to the location of Permian hydrothermal deposits. Thick broken line delimitates the Central Iberian Zone.

of allanites. The age of this fluid event may be broadly constrained to *ca.* 275Ma (Fig. 7), similar to the age of gold-bearing episyenites in the Villalcampo Shear Zone and barren episyenites in the SCS, both being consequence of a Permian large-scale crustal extension in Iberia. It is not ruled out that these fluids have been mobilized through planes related to the Juzbado-Penalva Shear Zone during a late reactivation of this megastructure.

CONCLUSIONS

U-Pb zircon ID-TIMS ages of vaugnerites from the Iberian Massif overlap with zircon and monazite U-Pb of granitoids and anatectic rocks in the same area, which implies that mantle melting (vaugnerites) and crustal melting (granites and anatectic rocks) are coeval. The advective heat input from the mantle, *i.e.* the heat carried by the vaugnerites, ultrapotassic and rocks of shoshonitic-affinity, is insufficient to account for the large-scale crustal melting. Instead, the pervasive anatexis of the area is related to the extensional regime that prevailed at 320-318Ma. In such a scenario, the quasi-isothermal decompression triggers anhydrous partial melting by mica-dehydration (crustal melts) in the crust and preferential melting of metasomatic domains in the upwelling lithospheric mantle (vaugnerites). Thus, even though vaugnerites, granites and anatectic melts are derived from different reservoirs

and may be petrogenetically entirely unrelated, they are coeval as the same process (large-scale crustal extension) controlled the production of the melts.

The U-Pb age of allanite is distinctly younger than the emplacement of the vaugnerite, implying that the U-Pb system of allanite may have been disturbed by subsolidus overprint during a later event at a lower temperature and pressure. The disturbance of the U-Pb system of allanite may have occurred at *ca*. 275Ma (Permian), *i.e*. a period characterized by an important hydrothermal activity in the Central Iberian Zone, with the formation of tungsten, gold deposits and episyenites.

ACKNOWLEDGMENTS

This work has been funded under the DGCYT project "Geochemical, tectonic and experimental approach of the crustal recycling processes and the mantle-crust interaction: Genesis and emplacement of the granitoids from the Tormes Dome" (CGL2004-06808-C04-04). F.J. López-Moro thanks Dr. F. Lucassen and Dr. J. Glodny for their assistance at the GeoForschungsZentrum Potsdam.

REFERENCES

Antona, F.J., 1991. Fluidos mineralizadores en los yacimientos de oro de Saucelle y El Cabaco (Salamanca). PhD thesis, University of Salamanca, Spain, 236pp.

Baumgartner, R., Romer, R.L., Moritz, R. Sallet, R., Chiaradia, M., 2006. Columbite-tantalite pegmatites from the Seridó Belt, NE Brazil: genetic constraints from U-Pb dating and Pb isotopes. The Canadian Mineralogist, 44, 69-86.

Bea, F., Montero, P., Talavera, C., Zinger, T., 2006. A revised Ordovician age for the oldest magmatism of Central Iberia: U-Pb ion-microprobe and LA-ICPMS dating of the Miranda do Douro orthogneiss. Geologica Acta, 4(3), 395-401.

Caballero, J.M., Casquet, C., Galindo, C., González-Casado, J.M., Pankhurst, R., Tornos, F., 1993. Geocronología por el método Rb-Sr de las episienitas de la Sierra de Guadarrama. Geogaceta, 13, 16-18.

Capdevila, R., Corretgé, L.G., Floor, P., 1973. Les granitoïdes varisques de la Meseta Ibérique. Bulletin de la Société Géologique de France, 15, 209-228.

Castro A, Corretgé, L.G., de la Rosa, J.D., Enrique, P., Martínez, F.J., Pascual, E., Lago, M., Arranz, E., Galé, C., Fernández, C., Donaire, T., López, S., 2002. Palaeozoic magmatism. In: Gibbons, W., Moreno, T. (eds.). The Geology of Spain. Geological Society, London, 117-153.

Castro, A., Corretgé, L.G., de la Rosa, J.D., Fernández, C., López, S., García-Moreno, O., Chacón, H., 2003. The appinite-migmatite complex of Sanabria, NW Iberian Massif, Spain. Journal of Petrology, 44, 1309-1344.

Chacón Muñoz, H., 2005. Caracterización geoquímica de la fase fluida en magmas de composición intermedia a básica. Aplicación al magmatismo apinítico de Sanabria y casos similares del Macizo Ibérico. PhD Thesis, University of Huelva, Spain, 379pp.

Escuder Viruete, J., Arenas, R., Martínez Catalán, J.R., 1994. Tectonothermal evolution associated with Variscan crustal extension in the Tormes Gneiss Dome (NW Salamanca, Iberian Massif, Spain). Tectonophysics, 238, 117-138.

Escuder Viruete, J., Indares, A., Arenas, R., 2000. P-T paths derived from garnet growth zoning in an extensional setting: an example from the Tormes Gneiss Dome (Iberian Massif, Spain). Journal of Petrology, 41, 1489-1515.

Ferreira, N., Castro, P., Pereira, E., Dias, G., Miranda, A., 2000. Syn-tectonic plutonism and Variscan anatexis of a Cadomian crust (Miranda do Douro region). In: Dias, G., Noronha, F., Ferreira, N. (eds.). Variscan plutonism in the Central Iberian Zone (Northern Portugal). Eurogranites 2000, Guide Book, Universidade do Minho, 183pp.

Foley, S., 1992. Vein-plus-wall-rock melting mechanisms in the lithosphere and the origin of potassic alkaline magmas. Lithos, 28, 435-453.

Fournet, J., 1861. Géologie Lyonnaise. Imprimerie De Barret. Lyon, France, 744pp.

García de los Ríos, J.I., 1981.Estudio petrológico-estructural de la región granítica situada al NE de Almeida (Provincia de Zamora). MSc Thesis, University of Salamanca, Spain, 70pp.

Gallastegui, G., 2005. Petrología del macizo granodiorítico de Bayo-Vigo (Provincia de Pontevedra, España). Serie Nova Terra, 26. Laboratorio Xeolóxico de Laxe. Área de Xeoloxía e Minería do Seminario de Estudos Galegos. Ediciós O Castro, La Coruña, Serie Nova Terra, 26, 414pp.

Gerstenberger, H., Haase, G., 1997. A highly effective emitter substance for mass spectrometric Pb isotope ratio determinations. Chemical Geology, 136, 309-312.

Gil Ibarguchi, J.I., 1982. Metamorfismo y plutonismo de la región de Muxía-Finisterre (NW, España). Corpus Geologicum Gallaeciae, 2ª Serie I, 253pp.

Gil Ibarguchi, J.I., Martinez, F.J., 1982. Petrology of garnet-cordierite-sillimanite gneisses from the El Tormes Thermal Dome, Iberian Hercynian Foldbelt (W Spain). Contributions to Mineralogy and Petrology, 80, 14-24.

González Clavijo, E., Díez Montes, A., 2008. Late Variscan processes in the Central Iberian Zone. The sub-vertical shear zones in Tormes Dome. Geotemas, 10, 445-448.

González Sánchez, M., 2016. Estudio de las principales rocas plutónicas empleadas en la construcción y restauración de monumentos en la ciudad de Salamanca. PhD Thesis, University of Salamanca, Spain, 351pp.

Gutiérrez-Alonso, G., Collins, A.S., Fernández-Suárez, J., Pastor-Galán, D., González-Clavijo, E., Jourdan, F., Weil, A.B., Johnston, S.T., 2015. Dating of lithospheric buckling: $^{40}Ar/^{39}Ar$ ages of syn-orocline strike-slip shear zones in northwestern Iberia. Tectonophysics, 643, 44-54.

Iglesias, M., Choukroune, P., 1980. Shear zones in the Iberian arc. Journal of Structural Geology, 2, 63-68.

Janousek, V., Holub, F.V., 2007. The causal link between HP–HT metamorphism and ultrapotassic magmatism in collisional orogens: case study from the Moldanubian Zone of the Bohemian Massif. The Proceedings of the Geologists' Association, 118, 75-86.

Krogh, T.E., 1973. A low-contamination method for hydrothermal decomposition of zircon and extraction of U and Pb for isotopic age determinations. Geochimica et Cosmochimica Acta, 37, 485-494.

López-Moro, F.J., 2000. Las rocas plutónicas calcoalcalinas y shoshoníticas del domo varisco del Tormes (centro-oeste español). Estudio mineralógico, geoquímico y petrogenético. PhD Thesis, Universidad de Salamanca, 441pp.

López-Moro, F.J., López-Plaza, M., 1998. Characterization and origin of the alkali feldspar of granitoid rocks from the Variscan Anatectic Tormes Dome. European Journal of Mineralogy, 10, 535-550.

López-Moro, F.J., López-Plaza, M., 2001. La asociación monzonítica del Domo Anatéctico del Tormes: geoquímica y petrogénesis. Estudios Geológicos, 57, 99-113.

López-Moro, F.J., López-Plaza, M., 2004a. Los anfíboles de las rocas básicas e intermedias de afinidad shoshonítica en el domo del Tormes. Stvdia Geologica Salmanticensia, 40, 31-55.

López-Moro, F.J., López-Plaza, M., 2004b. Los clinopiroxenos de las rocas ultrapotásicas y shoshoníticas (básicas e intermedias) del domo de Tormes. Un caso de reequilibrio subsolidus con una fase fluida. Stvdia Geologica Salmanticensia, 40, 11-29.

López-Moro, F.J., Moro, M.C., Timón, S.M., Cózar, J., 2007. Geochronology of gold deposits associated with Variscan granitoids in central west Iberia. In: Andrew, C.J., Borg, G. (eds.). Digging Deeper: Ninth Biennal Meeting of the Society for Geology Applied to Mineral Deposits, Dublin, Ireland. Proceedings, Irish Association for Economic Geology, 1, 385-388.

López-Moro, F.J., López-Plaza, M., Romer, R.L., 2012. Generation and emplacement of shear-related highly mobile crustal melts: the synkinematic leucogranites from the Variscan Tormes Dome, Western Spain. International Journal of Earth Sciences, 101, 1273-1298.

López-Moro, F.J., Moro, M.C., Timón, S.M., Cembranos, M.L., Cózar, J., 2013. Constraints regarding gold deposition in episyenites: the Permian episyenites associated with the Villalcampo Shear Zone, central western Spain. International Journal of Earth Sciences, 102, 721-744.

López-Moro, F.J., López-Plaza, M., Gutiérrez-Alonso, G., Fernández-Suárez, J., López-Carmona, A., Hofmann, M., Romer, R.L., 2017. Crustal melting and recycling: geochronology and sources of Variscan syn-kinematic anatectic granitoids of the Tormes Dome (Central Iberian Zone). A U–Pb LA-ICP-MS study. International Journal of Earth Sciences (Geologische Rundschau), 1-20, DOI: 10.1007/s00531-017-1483-8.

López-Plaza, M., 1982. Contribución al Conocimiento de la Dinámica de los Cuerpos Graníticos en la Penillanura Salmantino-Zamorana. PhD Thesis, Universidad de Salamanca, Spain, 333pp.

López-Plaza. M., López-Moro, F.J., 2004. El Domo del Tormes. In: Vera, J.A. (ed.). Geología de España. Sociedad Geológica Española-Instituto Geológico y Minero de España (SGE-IGME), Madrid, 100-101.

López-Plaza. M., López-Moro, F.J., 2008. The Tormes Dome. In: López-Plaza, M., López-Moro, F.J. (eds.). Eurogranites in Western Castilla y León, part II. University of Salamanca, Salamanca, 192pp.

López-Plaza. M., González Sánchez, M., García de Los Ríos Cobo, J.I., Cortázar Estíbaliz, J., Íñigo Íñigo, A.C., Vicente Tavera, S., López-Moro, F.J., 2007. La utilización de rocas vaugneríticas en los monumentos de Salamanca. Stvdia Geologica Salmanticensia, 43, 115-142.

López-Plaza. M., López-Moro, F.J., García de Los Ríos Cobo, J.I., 2012. Los plutones vaugneríticos del NE de Sayago, Zamora. In: López-Moro, F.J., López-Plaza. M., Vasallo Toranzo, L., Azofra, E., García de Los Ríos Cobo, J.I. (eds.). De los plutones a los monumentos. Un recorrido temático por la piedra del Este de Sayago (Zamora): El granito silicificado de Peñausende y la vaugnerita de Arcillo. Instituto de Estudios Zamoranos Florián de Ocampo, Diputación de Zamora, 302pp.

Ludwig, K.L., 2000. Isoplot/Ex. A Geochronological toolkit for Microsoft Excel. Berkeley Geochronology Center. Special publication Nº 1, 55pp.

McCaig, A.M., 1988. Deep fluid circulation in fault zones. Geology, 16, 867-870.

McCaig, A.M., Wickham, S.M., Taylor, H.P., 1990. Deep fluid circulation in alpine shear zones, Pyrenees, France: field and oxygen isotope studies. Contributions to Mineralogy and Petrology, 106, 41-60.

Michon, G., 1987. Les vaugnérites de l'Est du Massif Central Français: apport de l'analyse statisque multivariée à l'étude géochimique des éléments majeurs. Bulletin de la Société Géologique de France, 8, 591-600.

Molina, J.F., Montero, P., Bea, F., Scarrow, J.H., 2012. Anomalous xenocryst dispersion during tonalite-granodiorite crystal mush hybridization in the mid crust: Mineralogical and geochemical evidence from Variscan appinites (Avila Batholith, Central Iberia). Lithos, 153, 224-242.

Pereira, M.F., Díez Fernández, R., Gama, C., Hofmann, M., Gärtner, A., Linnemann, U., 2017. S-type granite generation and emplacement during a regional switch from extensional to contractional deformation (Central Iberian Zone, Iberian autochthonous domain, Variscan Orogeny). International Journal of Earth Sciences (Geologische Rundschau), 1-17, DOI: 10.1007/s00531-017-1488-3.

Poitrasson, F., 2002. In situ investigations of allanite hydrothermal alteration: examples from calc-alkaline and anorogenic granites of Corsica (southeast France). Contributions to Mineralogy and Petrology, 142, 485-500.

Prelević, D., Foley, S.F., 2007. Accretion of arc-oceanic lithospheric mantle in the Mediterranean: evidence from extremely high-Mg olivines and Cr-rich spinel inclusions in lamproites. Earth and Planetary Science Letters, 256, 120-135.

Prelević, D., Stracke, A., Foley, S.F., Romer, R.L., Conticelli, S., 2010. Hf isotope compositions of Mediterranean lamproites: mixing of melts from asthenosphere and crustally contaminated lithosphere. Lithos, 119, 297-312.

Prelević, D., Akal, C., Foley, S.F., Romer, R.L., Stracke, A., van den Bogaard, P., 2012. Ultrapotassic mafic rocks as geochemical proxies for post-collisional dynamics of orogenic lithospheric mantle: the case of southwestern Anatolia, Turkey. Journal of Petrology, 53, 1019-1055.

Prelević, D., Akal, C., Romer, R.L., Mertz-Kraus, R., Helvaci, C., 2015. Magmatic response to slab tearing: constraints from the Afyon Alkaline Volcanic Complex, western Turkey. Journal of Petrology, 56, 527-562.

Rodríguez, J., Gil Ibarguchi, I., Paquette, J., 2007. Variscan synchronous magmatism across the Iberian Massif: new U-Pb ages in granitoids from the Fisterra area (A Coruña, Spain) (In Spanish). XV Semana VI Congreso Ibérico, Vila Real, Portugal, 146-149.

Sabatier, H., 1991. Vaugnérites: Special Lamprophyre-derived mafic enclaves in some hercynian granites from Western and Central Europe. In: Didier, J. and Barbarin, B. (eds.). Enclaves and granite petrology. Developments in Petrology, 13, 63-81.

Scarrow, J.H., Molina, J.F., Bea, F., Montero, P., 2009. Within-plate calc-alkaline rocks: Insights from alkaline mafic magma-peraluminous crustal melt hybrid appinites of the Central Iberian Variscan continental collision. Lithos, 110, 50-64.

Schärer, U., 1984. The effect of initial ^{230}Th disequilibrium on young U-Pb ages: the Makalu case, Himalaya. Earth and Planetary Science Letters, 67, 191-204.

Selverstone, J., Morteani, G., Staude, J.M., 1991. Fluid channelling during ductile shearing: transformation of granodiorite into aluminous schist in the Tauern Window, eastern Alps. Journal of Metamorphic Geology, 9, 419-431.

Soder, C., Altherr, R., Romer, R.L., 2016. Mantle metasomatism at the edge of a retreating subduction zone: Late Miocene lamprophyres from the island of Kos, Greece. Journal of Petrology, 57, 1705-1728.

Steiger, R.H., Jäger, E., 1977. Subcommission of geochronology: Convention on the use of decay constants in geo- and cosmochronology. Earth and Planetary Science Letters, 36, 359-362.

Streit, J.E., Cox, S.F., 1998. Fluid infiltration and volume change during mid-crustal mylonitization of Proterozoic granite, King Island, Tasmania. Journal of Metamorphic Geology, 16, 197-212.

Talavera, C., Montero, P., Bea, F., Lodeiro, F. G., Whitehouse, M., 2013. U-Pb zircon geochronology of the Cambro-Ordovician metagranites and metavolcanic rocks of central and NW Iberia. International Journal of Earth Sciences, 102, 1-23.

Valverde-Vaquero, P., Díez Balda, M.A., Díez Montes, A., Downes, H., Escuder Viruete, J., González-Clavijo, E., Maluski, H., Rodríguez-Fernández, L.R., Rubio, F., Villar, P., 2007. The ''Hot Orogen'': two separate Variscan low-pressure metamorphic events in the Central Iberian Zone (Abstract 76). Mechanics of Variscan Orogeny: a modern view on orogenic research. Géologie de la France, Bureau de Recherche Géologique et Minières (BRGM), 2pp.

Vegas, N., Rodriguez, J., Cuevas, J., Siebel, W., Esteban, J.J., Tubía, J.M., Basei, M., 2011. The sphene-centered ocellar texture: An effect of grain-supported flow and melt migration in a hyperdense magma mush. The Journal of Geology, 119, 143-157.

Von Raumer, J.F., Finger, F., Veselá, P., Stampfli, G.M., 2014. Durbachites-Vaugnerites – a geodynamic marker in the central European Variscan orogeny. Terra Nova, 26, 85-95.

Whitney, D.L., Evans, B.W., 2010. Abbreviations for names of rock-forming minerals. American Mineralogist, 95, 185-187.

Manuscript received June 2017;
revision accepted November 2017;
published Online November 2017.